

Loop-Mediated Isothermal Amplification-Coupled Glass Nanopore Counting Toward Sensitive and Specific Nucleic Acid Testing

Zifan Tang,[†] Gihoon Choi,[†] Reza Nouri,[†] and Weihua Guan^{*,†,‡,§}

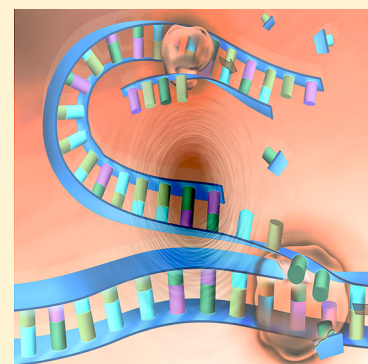
[†]Department of Electrical Engineering, Pennsylvania State University, University Park, Pennsylvania 16802, United States

[‡]Department of Biomedical Engineering, Pennsylvania State University, University Park, Pennsylvania 16802, United States

Supporting Information

ABSTRACT: Solid-state nanopores have shown great promise and achieved tremendous success in label-free single-molecule analysis. However, there are three common challenges in solid-state nanopore sensors, including the nanopore size variations from batch to batch that makes the interpretation of the sensing results difficult, the incorporation of sensor specificity, and the impractical analysis time at low analyte concentration due to diffusion-limited mass transport. Here, we demonstrate a novel loop-mediated isothermal amplification (LAMP)-coupled glass nanopore counting strategy that could effectively address these challenges. By using the glass nanopore in the counting mode (versus the sizing mode), the device fabrication challenge is considerably eased since it allows a certain degree of pore size variations and no surface functionalization is needed. The specific molecule replication effectively breaks the diffusion-limited mass transport thanks to the exponential growth of the target molecules. We show the LAMP-coupled glass nanopore counting has the potential to be used in a qualitative test as well as in a quantitative nucleic acid test. This approach lends itself to most amplification strategies as long as the target template is specifically replicated in numbers. The highly sensitive and specific sensing strategy would open a new avenue for solid-state nanopore sensors toward a new form of compact, rapid, low-cost nucleic acid testing at the point of care.

KEYWORDS: *Nanopores, single molecule, loop-mediated isothermal amplification, nucleic acid testing*



Due to its conceptual simplicity and label-free operations, nanopore sensors have attracted intense research interest in electronic single-molecule detection. The nanopore sensor is typically operated by applying a potential difference across the two chambers to electrophoretically drive charged biopolymers through the nanoscale orifice. The readout is a current time trace with dips corresponding to single-molecule translocation, usually called an event. Analysis of features within each identified event (e.g., dip magnitude, shape, and duration) provides the basis for interpreting the molecule length, shape, charge, and reactivity to the nanopore surface.¹ Among various nanopore types, due to their mechanical robustness, tunable size, and potential for integration and miniaturization, solid-state nanopores² made with silicon nitride,^{3–5} glass,^{6–8} and graphene⁹ have become a versatile analytical tool for analyzing nucleic acids and proteins.

While solid-state nanopores have achieved tremendous success, there exist three common challenges. The first is pore size variations from batch to batch. Despite significant advancement in solid-state nanopore fabrication techniques,¹⁰ repeatable pore size control remains challenging. Since the analyte is detected by the exclusion of ions from the sensing pore volumes, the pore size change would cause the sensing signal varying from one experiment to the other, making the interpretation of the sensing results difficult. The second is the nanopore sensor specificity. The specificity was usually

encoded into the dwell time or current dip shapes. A common approach for achieving the specificity is through introducing specific binding sites on the nanopore wall surface.^{11,12} However, controlling the location and number of binding sites within the nanopore sensing volume is not without challenges. The additional steps of surface functionalization could limit the device yield.¹³ In addition, a specifically modified nanopore means that nanopores can only be used for a fixed target without being generally applicable. Another approach for introducing the specificity is through specific probe molecules. For example, engineered double-strand DNA carriers were used for sensing specific proteins^{14,15} and specific DNAs.¹⁶ The third challenge is the prolonged sensor response time at low analyte concentrations.^{2,17} Although the nanopore sensor itself has single molecule sensitivity, the diffusion-limited mass transport in nanopore sensors could severely impact the sensor response time.^{17–19} It was estimated that if the analyte concentration is subpicomolar, it will take more than 1 h to observe a single event.²⁰

To extend the capabilities of solid-state nanopores and realize practical devices, alternative sensing strategies are highly desirable. One such strategy is to increase the number of

Received: July 24, 2019

Revised: October 21, 2019

Published: October 28, 2019

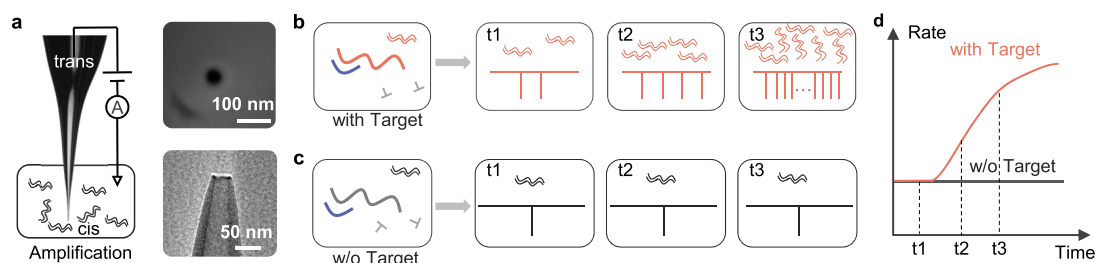


Figure 1. Illustration of the working principle of nanopore counting of amplicons. (a) Schematic measurement setup as well as the SEM and TEM of the glass nanopore. Amplicons are electrophoretically driven through the glass nanopore one by one, resulting in discernible events of the ionic current blockade. The event rate is proportional to the amplicon concentration. (b) Events in a positive target case. (c) Events in a negative target case. (d) Schematic event rate as a function of amplification time (or cycle).

specific target molecules present. In fact, target molecule replication was a mature and proven strategy in nucleic acid amplification tests (NAATs). As one of the most sensitive methods available, NAATs have a wide range of applications ranging from infectious disease diagnosis, food pathogen screening, and forensic investigations to homeland security. NAAT employs enzymatic polymerization reaction in which a few copies of templates (low analyte concentration) can be replicated specifically into a large number of amplicons (high analyte concentration). There have been a variety of molecule replication strategies developed. In addition to the traditional polymerase chain reaction (PCR), isothermal methods such as loop-mediated isothermal amplification (LAMP),^{21,22} nucleic acid sequence-based amplification (NASBA),²³ and recombinase polymerase amplification (RPA)²⁴ have shown great promise for field use since they do not require thermocyclers and often are very fast.

In this work, we reported a LAMP-coupled glass nanopore counting method for highly sensitive and specific nucleic acid testing. By using the glass nanopore in its simplest form of event counting (versus analyzing the shape features of the current blockade), the device fabrication challenge is considerably eased since it allows a certain degree of pore size variation (as long as it can still resolve single molecules) and requires no surface functionalization. The LAMP replication simultaneously offers the requisite specificity and effectively breaks the diffusion-limited mass transport at low analyte concentration thanks to the exponential growth of the target molecules. We examined the ability of the glass nanopore to capture the LAMP reaction dynamics. We found that LAMP-coupled glass nanopore counting has the potential to be used in a qualitative as well as quantitative test. The amplification-coupled nanopore counting approach would open a new avenue toward compact and robust electronic nucleic acid testing at the point of care.

Results and Discussion. Working Principle. As one of the resistive pulse sensors, nanopores were usually used for two purposes: size determination^{16,25} and counting.^{26–28} While analyte sizing is sensitive to the pore size, analyte counting is less so. Our approach used the glass nanopore in its simplest function of counting to quantify the amplicon abundance (Figure 1), which was conventionally quantified by the fluorescence sensing using probes like TaqMan or intercalating dye like SYBR Green. Note that batch-to-batch precise glass nanopore size control is not required in the counting mode as long as it is able to resolve the single molecule event. The glass nanopore used in our experiment is typically 10 nm in diameter. Existing theory²⁹ and experiment²⁷ have shown that the DNA molar concentration (C in mol/m³) is related to the

event rate (R in s⁻¹). Therefore, it is possible to infer the amplicon concentration by measuring the event rate. Note that we used the term “event rate” rather than “capture rate” to describe the counting rate of molecules, because “capture rate” could refer to concentration normalized rate^{29,30} in previous studies (Note S1, Supporting Information). Figure 1a shows the schematic diagram of the experimental setup with conically shaped glass nanopore as the single molecule counting device. The amplification reaction is sealed with mineral oil to avoid evaporation and cross-contamination. For a positive reaction (Figure 1b), the increase of amplicons manifests itself as the increase of the event rate. For the negative reaction (Figure 1c), the event rate remains unchanged or undetectable. The rate determined at certain time spots during the amplification is an electronic measurement of the corresponding amplicon concentrations (Figure 1d).

Before the amplification experiment, we first addressed whether the single molecule counting rate could be used as a reliable readout for DNA concentration in our glass nanopores. We performed studies on 5 kbp DNAs with a serial of concentrations ranging from 12 to 60 pM. A quick look at the current time traces in Figure 2a shows that the interarrival time between two events becomes shorter when concentration increases; in other words, the event rate is faster at higher concentration. The extracted interarrival time distribution

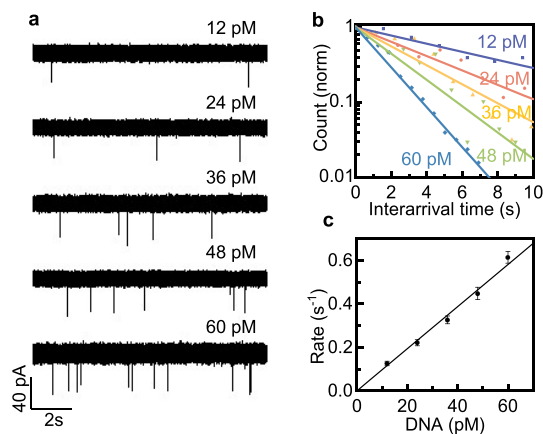


Figure 2. Continuous recordings of current trace under 500 mV bias with 5 kbp-DNA through glass nanopore at 1 M KCl in Tris-EDTA-buffer solution. (a) Segments of the current trace at different DNA concentrations. (b) The normalized probability distribution of the interarrival time at different concentrations, with corresponding exponential fits. (c) The average event rate as a function of DNA concentration, showing a linear dependence ($R^2 = 0.985$).

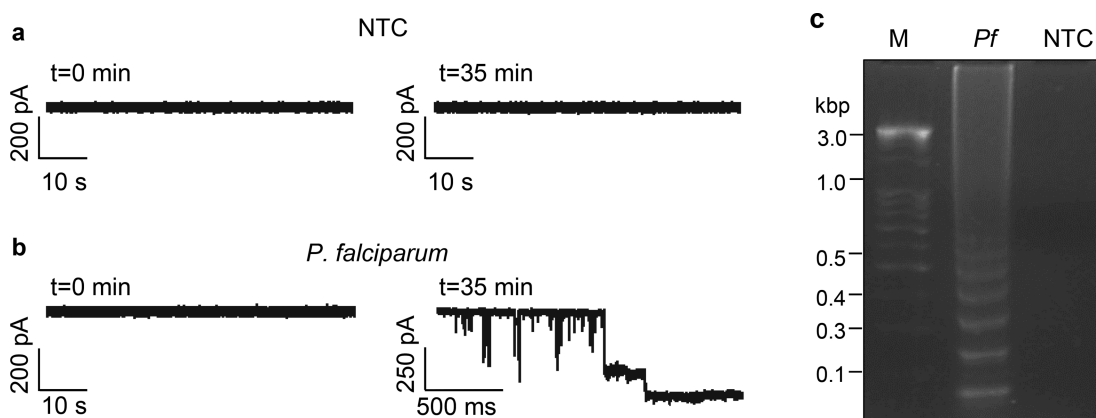


Figure 3. Concept validation of nanopore counting of amplicons. Time traces for (a) negative NTC and (b) positive control before and after the 35 min LAMP reaction. The clogging issue was observed in the positive controls. (c) Gel electrophoresis image of the LAMP products (2% agarose gel).

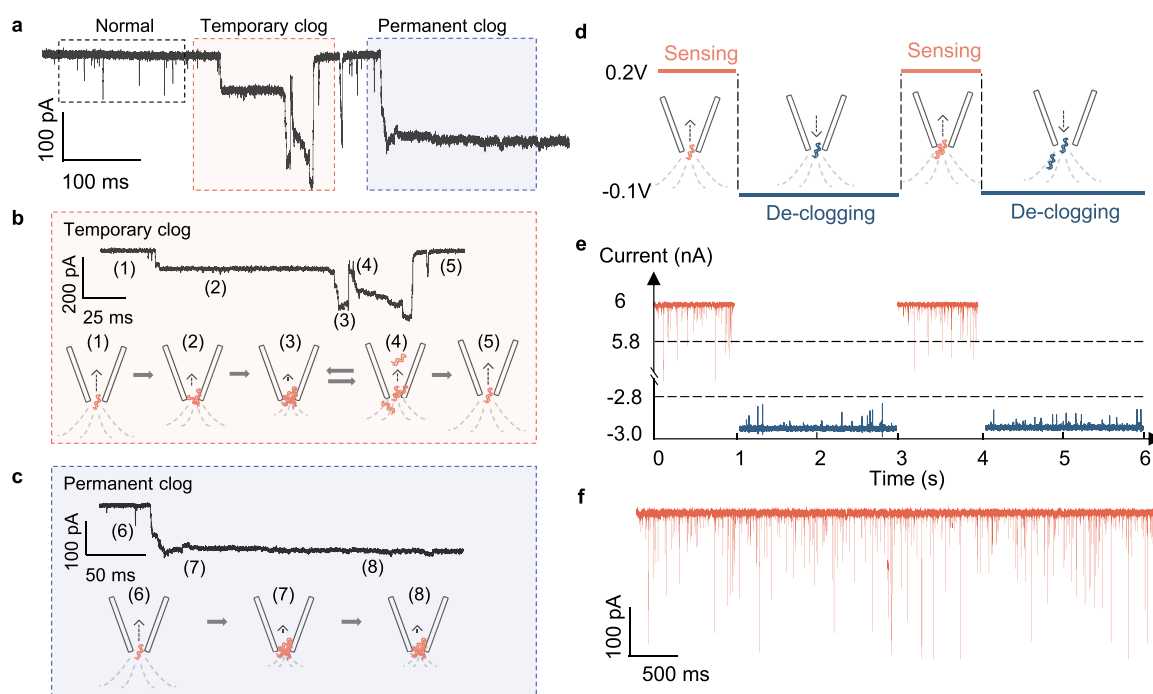


Figure 4. Resolving the nanopore clogging by voltage cycling scheme. (a) A representative current trace showing normal, temporary clog, and permanent clog. (b) Expanded view of the temporary clog. (c) Expanded view of the permanent clog. (d) Illustration of the voltage cycling scheme. The voltage is cycled between 1 s of 200 mV for sensing and 2 s of -100 mV for declogging. (e) A typical current trace using the voltage cycling scheme. (f) Reconstructed 5 s current trace by sequentially combining the current obtained under the 200 mV sensing voltage. A total of 487 events could be identified without clogging issue.

shows a remarkable exponential distribution for each concentration (Figure 2b), indicating a Poisson process, consistent with previous observations in the silicon nitride nanopore.³¹ Each concentration case was then fitted with an exponential distribution, $P(t) = \lambda e^{-\lambda t}$, where λ is the expected single-molecule event rate. Figure 2c shows the single-molecule event rate as a function of the DNA concentrations. Note that a limited concentration range was probed in Figure 2. The average molecular distance ranges from 3 to 5.2 μm , and therefore interactions between molecules are negligible (Note S2, Supporting Information). As a result, molecule concentration is indeed expected to be linearly related to the event rate.²⁹

Concept Validation. As an alternative to thermal-cycling based PCR method, isothermal assays such as LAMP are very

promising for developing a sensitive molecular test in resource-limited settings.^{21,22,32,33} We set out to test if the glass nanopore could detect the end product of the LAMP reaction. First, we tested the no-template control (NTC) sample when it was freshly prepared ($t = 0$ min) and after 35 min of LAMP reaction. As shown in Figure 3a, no events were observed for 60 s of recording. This confirmed the LAMP reagents, such as deoxynucleotide triphosphates (dNTPs), polymerase enzyme, and primers, were not detectable by the glass nanopore. This is likely because the 10 nm-sized nanopore is too big for these background targets. After confirming the background master mix did not produce measurable events, we continued to test the positive control sample with *Plasmodium falciparum* genomic DNA. As shown in Figure 3b, no detectable events were noticeable before the LAMP reaction ($t = 0$ min), further

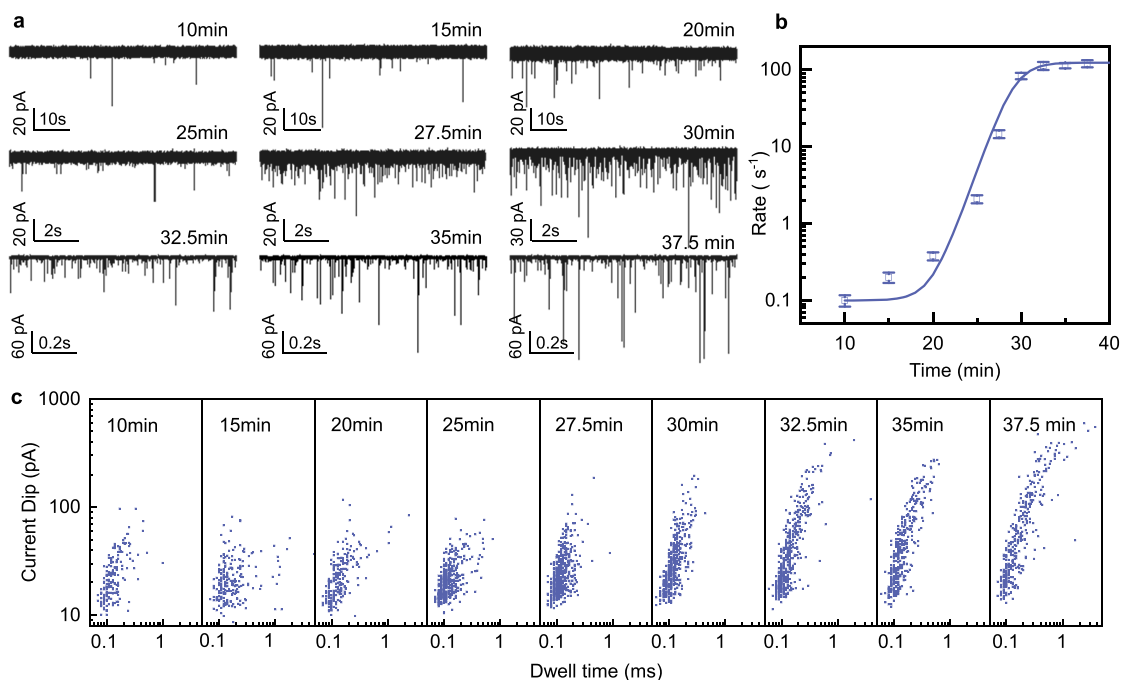


Figure 5. Nanopore counting to probe the LAMP reaction dynamics. (a) Current traces at various amplification times. (b) The event rate as a function of the amplification time. The event rate increased exponentially before reaching a saturated level. The solid line is fitting to the logistic growth model ($R_L = 0.1 \text{ s}^{-1}$, $R_H = 123.2 \text{ s}^{-1}$, $\beta = 0.75 \text{ min}^{-1}$, and $t_0 = 29.2 \text{ min}$). (c) Scatter plots showing current dip magnitude vs dwell time at various reaction times.

confirming the LAMP master mix does not interfere with the measurement. However, after 35 min of LAMP reaction of this positive control sample, clear events were immediately observable in the first second of measurement. Figure 3c shows the gel image of the final LAMP products for both positive and negative controls. The sharp contrast in the event rate between Figure 3a and Figure 3b confirms the glass nanopore is able to detect the LAMP end products qualitatively.

Resolving the Pore Clogging by Voltage Cycling Scheme. Nanopore clogging is a common issue during long-term measurements. In testing the end product of the positive control sample (Figure 3b), two abrupt current drops sequentially occurred and the current stopped returning to its baseline after only a few seconds of the continuous current recording. A careful examination of the current time trace reveals that the event rate is about 68 s^{-1} before the drop, much higher than the rate shown in Figure 2, indicating the amplicon concentration is very high. This is not surprising because the number of amplicons grows significantly during the LAMP reaction. At this high concentration, the DNAs are highly likely to be jammed near the nanopore entrance, leading to partial or full clogging of the nanopore. This jamming effect³⁴ caused a potential problem for reliable event rate determination for long-term measurement.

Another more representative current time trace from the LAMP end product was shown in Figure 4a, which contains a full picture of different translocation scenarios. The normal DNA translocation through the nanopore usually takes about $500 \mu\text{s}$. The temporary clog case is expanded in Figure 4b. Segment 1 has the baseline current corresponding to the open nanopore condition. The ionic current shifts down by around 50 pA for segment 2, indicating a partial clogging of the nanopore. The baseline current drops another 100 pA in

segment 3 with more DNAs coming at the nanopore and becomes jammed. However, these temporary jams eventually get cleared after some time, and the baseline current returns to its open-pore value (segment 5). In contrast, the permanent clog case is magnified in Figure 4c, in which the baseline current stopped coming back to its open-pore level.

Both temporary and permanent clog issues will negatively impact the nanopore's capability to count the amplicons continuously. To resolve this issue, we developed a voltage cycling scheme for long-term recording (Figure 4d), similar to a previously reported approach.³⁵ The duration of the positively applied voltage (200 mV) that drives the DNA into the glass nanopore was typically limited to 1 s , in which the single molecule events were recorded. This was followed by a declogging step using a negative voltage (-100 mV) with a typical duration of 2 s to allow DNAs to drift in reverse direction and to rerandomize via diffusion. Figure 4e shows the current time trace in two consecutive voltage cycles on the same LAMP product. Figure 4f shows the overlay of the current traces over 5 s with a total of 487 events. As shown, the reconstructed sensing current shows no baseline shift, which suggests the voltage cycling scheme can resolve the clogging issue and is suitable for long-time measurement. It is noteworthy that under the voltage cycling scheme, we did not observe any permanent clog issue for all hour-long experiments we performed. All the following data presented were generated under this scheme after reconstruction.

Probing LAMP Reaction Dynamics. After establishing a reliable approach for rate measurement, we tested if the nanopore counting could resolve the LAMP dynamics. Using the *P. falciparum* genomic DNA, LAMP assays were performed for a duration ranging from 10 to 37.5 min at $65 \text{ }^\circ\text{C}$, the product of which is counted using the same glass nanopore. The event rate at 95% confidence interval was calculated as (n

$\pm 1.96(n)^{1/2}/T$ since these events follow the Poisson process,^{8,36} where n is the number of events observed, and T is the total elapsed time. The relative uncertainty of inferring the rate R is proportional to $n^{-1/2}$. For each reaction time, we counted at least 150 events to ensure measurement uncertainty <8%. Figure 5a shows segments of the current time trace for each reaction time (see Figure S1 for all-time current traces). It is evident that the event rate increases with extended reaction time (note the scale difference among the plots).

Figure 5b shows the extracted event rate as a function of LAMP reaction time. The rate shows more than a 3 orders of magnitude increase when the reaction time goes from 10 to 37.5 min. Interestingly, the event rate (which is a readout of the LAMP amplicon quantities) versus the reaction time can be fitted remarkably well with a logistic growth model (Note S3, Supporting Information):

$$R(t) = R_L + \frac{R_H - R_L}{1 + e^{-\beta(t-t_0)}} \quad (1)$$

where R_L and R_H are the low and high bound of the event rate, respectively, t_0 is the time when the growth rate is at maximum, and β is a measure of the maximum steepness of amplification rate at the exponential growth stage. The logistic growth model is widely used to describe the population's growth rate decreases as population size approaches its carrying capacity imposed by limited resources.³⁷ The agreement to the logistic growth model suggests the LAMP cycling reaction could not sustain a constant exponential growth and is indeed subject to the limited number of dNTPs, polymerase enzymes, and primers available in the 25 μ L LAMP reaction mix.

Another interesting feature observed in Figure 5a is the widely distributed current dip magnitude and dwell time for single molecule events. Figure 5c shows the current dip–dwell time scatter plot at each LAMP reaction time. As the amplification time increases, a substantial increase of population with higher current dip and longer dwell time was observed, indicating longer DNAs are produced when the reaction continues. This is indeed expected for the LAMP reaction, in which the final product obtained is a mixture of stem-loop DNA with various stem lengths and various cauliflower-like structures with multiple loops. The structures are formed by annealing between alternatively inverted repeats of the target sequence in the same strand.^{21,22}

Qualitative Testing. To demonstrate the potential utility of the LAMP-coupled nanopore counting approach for qualitative (yes/no) specific nucleic acid testing, we examined two of the most spread species of malaria: *P. falciparum* (*Pf*) and *Plasmodium vivax* (*Pv*). Before the nanopore experiment, we first validated the *Pf*- and *Pv*-specific LAMP primer sets in a benchtop real-time PCR instrument (Bio-Rad, Figure S2). Each species-specific assay was then tested with three different types of samples (*Pf*, *Pv*, and NTC). We used the nanopore to analyze the end product of the LAMP assay after 35 min of reaction at 65 °C. Figure 6a,b shows the resulting current time traces for *Pf*-specific assay and *Pv*-specific assay, respectively. The events with a rate of 31.2 s⁻¹ (*Pf* in *Pf*-specific assay) and 8.5 s⁻¹ (*Pv* in *Pv*-specific assay) were observed when the assays match with the intended species. No cross-reactivity was observed. To further validate that the signal observed was not due to the random noise, we performed gel electrophoresis in 2% agarose gel. As shown in Figure 6c,d, clear ladder-like patterns with multiple bands of different molecular sizes were observed due to the stem-loop DNA structures with several

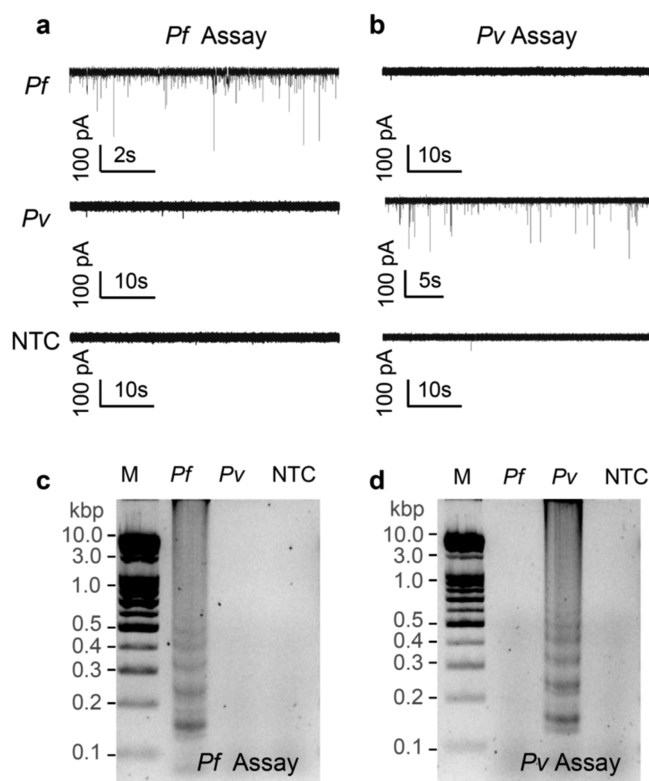


Figure 6. Qualitative-specific nucleic acid testing using the nanopore-LAMP. (a) Current traces obtained from nanopore reading for *Pf*-specific assay and (b) for *Pv*-specific assay. The event rate difference between the positive and the negative is evident. (c) Gel electrophoresis image (2% agarose gel) for *Pf*-specific assay and (d) for *Pv*-specific assay.

inverted repeats within LAMP amplicons.^{21,22} In contrast, no bands were observed in the nonspecific and NTC reactions.

Quantitative Testing. To evaluate the potential quantitative application of the nanopore counting platform, we performed the nanopore-LAMP assay on the mitochondrial gene by using a 10-fold serial dilution of purified *P. falciparum* genomic DNA. The nanopore-LAMP performance (Figure 7a) is benchmarked to the tube-based quantitative LAMP (qLAMP, Figure 7b) on a benchtop real-time PCR instrument using calcein as an indicator. Both the fluorescence-based method and the nanopore method show the expected right-shift of the amplification curve when reducing the gene copy numbers. The event rate data at different time spots are summarized in Table S1. In addition, as shown in Figure 7a, the event rate results from all diluted samples tested by the nanopore can be fitted remarkably well by the logistic growth model (with all $R^2 > 0.95$, Table S2). Figure 7c shows the extracted standard curves from both the nanopore and fluorescence methods. The threshold time is determined by the time corresponding to the reading of 500 RFU in the fluorescence method and 1 s⁻¹ in the nanopore method, respectively. The amplification over a range of serially diluted DNA samples showed excellent linearity in both methods ($R^2 = 0.98$ for fluorescence method and $R^2 = 0.99$ for nanopore method). The linearity in the nanopore method suggests it could be used for quantitative analysis of DNA. The different slope between the nanopore-LAMP and the benchtop thermal cycled-based LAMP is likely due to setup difference in the thermal and detection dynamics.

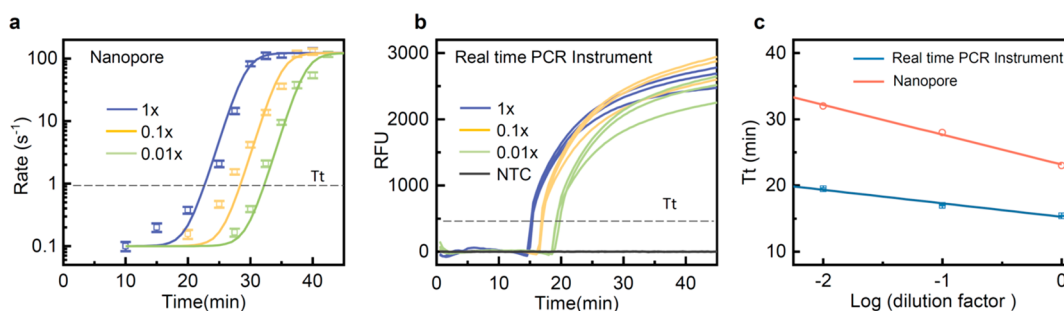


Figure 7. Comparison between the nanopore method and fluorescence-based method. (a) The results acquired from the nanopore detection. The solid lines were fittings to the logistic function (with fitting parameters summarized in Table S2). 1 \times , 0.1 \times , and 0.01 \times denote the dilution factors of the templates. 1 \times is equivalent to 100 ng/ μ L *Pf* genomic DNAs. (b) Amplification curves obtained from the fluorescence method using benchtop real-time PCR machine. (NTC: no template controls.) (c) Standard curves extracted from the nanopore platform and the fluorescence platform. The linearity in the nanopore method suggests it could be used for quantitative analysis of DNA.

Limit of Detection Considerations. While the limit of detection (LoD) was not experimentally explored as it is highly assay dependent, the LoD is impacted by two factors in nanopore counting. The first is the false positive rate when no amplicons exist, similar to the dark count rate in the single photon counters.³⁸ The false detection events are due to the noise in the testing apparatus as well as the background reagents. In our experiment, the false positive rate when testing the NTC sample is <0.01 during a 60 min test. The second factor is the Poisson noise during the counting. Since the relative uncertainty of inferring the rate is proportional to $n^{-1/2}$, a large enough event number (n) should be recorded to establish a sufficiently robust statistical basis.³⁹ Assuming a minimal event number n and a practical measurement time of T , a minimal event rate n/T is required, corresponding to the lower bound of detectable amplicons. In our study, we use 0.1 s^{-1} as minimal event rate so that we can obtain at least 10 events during a 100 s-long test. Future work could incorporate multiple parallel nanopores^{40,41} to improve the time resolution toward the real-time analysis.

Conclusions. In summary, our findings demonstrated the effectiveness of using a single-molecule-counting glass nanopore to probe the number of specifically replicated amplicons from the loop-mediated isothermal amplification. We show that the nanopore counting approach can capture the DNA replication dynamics in the LAMP and has the potential to be used in a qualitative as well as a quantitative nucleic acid test. The LAMP-coupled glass nanopore counting strategy addressed common challenges in solid-state nanopore sensors regarding the batch-to-batch nanopore size variation, the specificity, and the prolonged sensor response time at low analyte concentrations. By keeping the nanopore as simple as possible and coding the specificity information into the molecule numbers, the LAMP-coupled glass nanopore counting method provides a promising optics-free method for highly sensitive and specific nucleic acid testing at the point of care. While this work focused on the LAMP and the glass nanopore, we believe the amplification-coupled nanopore counting approach could be well extended to other molecule replication strategies and other solid-state nanopore types.

Methods. Materials and Chemicals. Quartz capillaries with inner and outer diameter of 0.5 and 1 mm were used in our experiment (Sutter Instrument, USA). Pipette holder (QSW-T10N) was purchased from Warner Instruments. Ag/AgCl electrodes were homemade with 0.2 mm Ag wires (Warner Instruments, USA). Microinjector with 34 gauge was

purchased from World Precision Instruments. 5 kbp DNA (0.5 μ g/ μ L) were purchased from ThermoFisher. KCl and Tris-EDTA-buffer solution (pH 8.0) were purchased from Sigma-Aldrich. All solutions were filtered with a 0.2 μ m syringe filter (Whatman). Mineral oil was purchased from Sigma-Aldrich. The *Pf* genomic DNAs (100 ng/ μ L) and *Pv* genomic DNAs (4.7 ng/ μ L) were gifts from Dr. Cui's lab at Penn State, extracted by phenol-chloroform based procedure.

LAMP Assay. The LAMP reaction mix (25 μ L) contains isothermal buffer (20 mM Tris-HCl, 10 mM $(NH_4)_2SO_4$, 50 mM KCl, 2 mM $MgSO_4$, 0.1% Tween 20, pH 8.8), PCR grade H_2O , $MgSO_4$ (7 mM), $MnCl_2$ (0.75 mM), calcein (25 μ M), deoxyribonucleotide triphosphates (dNTPs, 1.4 mM), Bst 2.0 DNA polymerase, DNA template, and primer sets (0.2 mM F3 and B3c, 1.6 mM FIP and BIP, 0.8 mM LPF and LPB). Table S3 shows the reagent recipe for the LAMP assay. The *Pf*-specific and *Pv*-specific primer sets are listed in Table S4. The LAMP assay was performed at a constant temperature of 65 $^\circ$ C.

Glass nanopore fabrication. The quartz capillaries were cleaned by piranha for 30 min to remove any organic contaminants and then repeatedly rinsed with DI water and dried in an oven at 120 $^\circ$ C for 15 min. The capillary was pulled by a laser pipet puller (P-2000, Sutter Instruments, USA) using a two-line program: (1) Heat 750, Filament 5, Velocity 50, Delay140, and Pull 50; (2) Heat 710, Filament 4, Velocity 30, Delay 155, and Pull 215. This recipe typically produces a nanopore size around 10 nm. Despite known batch-to-batch variations in size, the counting method is valid as long as the nanopore can resolve the single molecule event.

I-V, SEM, and TEM Characterization. The nanopore conductance was measured by taking a standard $I-V$ curve in 1 M KCl buffered with Tris-EDTA. Typical conductance of the fabricated nanopore is in the range of 20 ± 10 nS (Figure S3). For SEM imaging, 5 nm of iridium was sputtered onto the nanopore surface to prevent drifts caused by charging. SEM imaging was then performed under a working distance between 3 and 5 mm, magnifications of 88,415, beam currents of 2.5 pA, and an acceleration voltage of 3 kV. TEM characterization was also performed to obtain detailed information for the nanopore geometry.

Electrical Recording and Data Analysis. A constant voltage was applied across the nanopore constriction with a 6363 DAQ card (National Instruments, USA). The ionic current traces were recorded by an amplifier (Axopatch 200B, Molecular Device, USA). The analog output of the amplifier was sampled

with the 6363 DAQ card and a customized data acquisition software (LabVIEW). The sampling rate for the measurement was 100 kHz. The signal was low-pass filtered at 10 kHz. The measurement system was inside a homemade Faraday cage to shield the environment noise. We also analyzed the noise performance of the ionic current measurement (Figure S4). Typical RMS noise in our experiments is around 4.2 pA, low enough to distinguish the typical single molecule events with dip magnitude >10 pA. Our noise performance was comparable to these in the previous studies.²⁰ A custom-built MATLAB (MathWorks) program was developed to reconstruct the sensing data and to analyze the event rate, current dip duration, and depth for the single molecule events.

Nanopore-LAMP Experiment. The LAMP master mix (24 μL) and the target template (1 μL) was dispensed into the PCR tube, with an additional 25 μL of mineral oil added to prevent evaporation and cross-contamination. The PCR tube was placed in a dry block incubator preheated at 65 °C. The LAMP reaction was terminated at different times by heating at 95 °C for 5 min. The product solution was adjusted to 1 M salt concentration for nanopore measurement. The same glass nanopore was used for all samples amplified at various times. To ensure the signal observed was not due to spurious amplification, we performed the gel electrophoresis in 2% agarose after the amplification.

■ ASSOCIATED CONTENT

Supporting Information

The Supporting Information is available free of charge on the ACS Publications website at DOI: 10.1021/acs.nanolett.9b03040.

Detailed descriptions of mixed-use of capture rate and translocation rate, molecular distance estimation, logistic growth model, all current traces, LAMP assays validation in benchtop real-time PCR machine, nanopore I - V and noise characterization, extracted event rate after the specific LAMP reaction time, parameters for logistic function fitting, LAMP assay reagent setup and primer sets (PDF)

■ AUTHOR INFORMATION

Corresponding Author

*E-mail: wzg111@psu.edu.

ORCID

Weihua Guan: 0000-0002-8435-9672

Author Contributions

W.G. conceived the concept and supervised the study. T.Z. designed and carried out the nanopore fabrication and sensing experiment. G.C. performed the LAMP assay. T.Z., R.N., and W.G. analyzed the data. W.G. and T.Z. cowrote the manuscript and discussed with all other authors.

Notes

The authors declare no competing financial interest.

■ ACKNOWLEDGMENTS

The authors thank Dr. Jun Miao and Xiaolian Li for providing the malaria genomic DNAs and Tae-Jung Chung for electrophoresis gel imaging. This work supported by the National Science Foundation under grant nos. 1710831, 1902503, and 1912410. Any opinions, findings, and conclusions or recommendations expressed in this work are those

of the authors and do not necessarily reflect the views of the National Science Foundation. W.G. acknowledges the support from the Penn State Startup Fund.

■ REFERENCES

- (1) Miles, B. N.; Ivanov, A. P.; Wilson, K. A.; Dogan, F.; Japrun, D.; Edel, J. B. Single molecule sensing with solid-state nanopores: novel materials, methods, and applications. *Chem. Soc. Rev.* **2013**, *42* (1), 15–28.
- (2) Albrecht, T. Single-Molecule Analysis with Solid-State Nanopores. *Annu. Rev. Anal. Chem.* **2019**, *12* (1), 371–387.
- (3) Li, J. L.; Gershow, M.; Stein, D.; Brandin, E.; Golovchenko, J. A. DNA molecules and configurations in a solid-state nanopore microscope. *Nat. Mater.* **2003**, *2* (9), 611–615.
- (4) Yamazaki, H.; Hu, R.; Zhao, Q.; Wanunu, M. Photothermally Assisted Thinning of Silicon Nitride Membranes for Ultrathin Asymmetric Nanopores. *ACS Nano* **2018**, *12* (12), 12472–12481.
- (5) Roshan, K. A.; Tang, Z.; Guan, W. High fidelity moving Z-score based controlled breakdown fabrication of solid-state nanopore. *Nanotechnology* **2019**, *30* (9), 095502.
- (6) Steinbock, L. J.; Bulushev, R. D.; Krishnan, S.; Raillon, C.; Radenovic, A. DNA translocation through low-noise glass nanopores. *ACS Nano* **2013**, *7* (12), 11255–11262.
- (7) Bell, N. A.; Muthukumar, M.; Keyser, U. F. Translocation frequency of double-stranded DNA through a solid-state nanopore. *Phys. Rev. E: Stat. Phys., Plasmas, Fluids, Relat. Interdiscip. Top.* **2016**, *93* (2), 022401.
- (8) Nouri, R.; Tang, Z.; Guan, W. Calibration-Free Nanopore Digital Counting of Single Molecules. *Anal. Chem.* **2019**, *91* (17), 11178–11184.
- (9) Garaj, S.; Hubbard, W.; Reina, A.; Kong, J.; Branton, D.; Golovchenko, J. A. Graphene as a subnanometre trans-electrode membrane. *Nature* **2010**, *467* (7312), 190–193.
- (10) Li, J.; Stein, D.; McMullan, C.; Branton, D.; Aziz, M. J.; Golovchenko, J. A. Ion-beam sculpting at nanometre length scales. *Nature* **2001**, *412* (6843), 166–169.
- (11) Wei, R. S.; Gatterdam, V.; Wieneke, R.; Tampe, R.; Rant, U. Stochastic sensing of proteins with receptor-modified solid-state nanopores. *Nat. Nanotechnol.* **2012**, *7* (4), 257–263.
- (12) Iqbal, S. M.; Akin, D.; Bashir, R. Solid-state nanopore channels with DNA selectivity. *Nat. Nanotechnol.* **2007**, *2* (4), 243.
- (13) Keyser, U. F. Enhancing nanopore sensing with DNA nanotechnology. *Nat. Nanotechnol.* **2016**, *11* (2), 106–108.
- (14) Sze, J. Y. Y.; Ivanov, A. P.; Cass, A. E. G.; Edel, J. B. Single molecule multiplexed nanopore protein screening in human serum using aptamer modified DNA carriers. *Nat. Commun.* **2017**, *8* (1), 1552.
- (15) Bell, N. A. W.; Keyser, U. F. Specific Protein Detection Using Designed DNA Carriers and Nanopores. *J. Am. Chem. Soc.* **2015**, *137* (5), 2035–2041.
- (16) Kong, J. L.; Zhu, J. B.; Keyser, U. F. Single molecule based SNP detection using designed DNA carriers and solid-state nanopores. *Chem. Commun.* **2017**, *53* (2), 436–439.
- (17) Wu, Y. F.; Tilley, R. D.; Gooding, J. J. Challenges and Solutions in Developing Ultrasensitive Biosensors. *J. Am. Chem. Soc.* **2019**, *141* (3), 1162–1170.
- (18) Gooding, J. J.; Gaus, K. Single-Molecule Sensors: Challenges and Opportunities for Quantitative Analysis. *Angew. Chem., Int. Ed.* **2016**, *55* (38), 11354–11366.
- (19) Wanunu, M.; Morrison, W.; Rabin, Y.; Grosberg, A. Y.; Meller, A. Electrostatic focusing of unlabelled DNA into nanoscale pores using a salt gradient. *Nat. Nanotechnol.* **2010**, *5* (2), 160–5.
- (20) Freedman, K. J.; Otto, L. M.; Ivanov, A. P.; Barik, A.; Oh, S.-H.; Edel, J. B. Nanopore sensing at ultra-low concentrations using single-molecule dielectrophoretic trapping. *Nat. Commun.* **2016**, *7*, 10217.
- (21) Notomi, T.; Okayama, H.; Masubuchi, H.; Yonekawa, T.; Watanabe, K.; Amino, N.; Hase, T. Loop-mediated isothermal amplification of DNA. *Nucleic acids research* **2000**, *28* (12), No. e63.

(22) Tomita, N.; Mori, Y.; Kanda, H.; Notomi, T. Loop-mediated isothermal amplification (LAMP) of gene sequences and simple visual detection of products. *Nat. Protoc.* **2008**, *3* (5), 877.

(23) Ma, Y. L.; Teng, F. Y.; Libera, M. Solid-Phase Nucleic Acid Sequence-Based Amplification and Length-Scale Effects during RNA Amplification. *Anal. Chem.* **2018**, *90* (11), 6532–6539.

(24) Ahn, H.; Batule, B. S.; Seok, Y.; Kim, M. G. Single-Step Recombinase Polymerase Amplification Assay Based on a Paper Chip for Simultaneous Detection of Multiple Foodborne Pathogens. *Anal. Chem.* **2018**, *90* (17), 10211–10216.

(25) Venta, K.; Shemer, G.; Puster, M.; Rodriguez-Manzo, J. A.; Balan, A.; Rosenstein, J. K.; Shepard, K.; Drndic, M. Differentiation of Short, Single-Stranded DNA Homopolymers in Solid-State Nanopores. *ACS Nano* **2013**, *7* (5), 4629–4636.

(26) Jin, Q.; Fleming, A. M.; Johnson, R. P.; Ding, Y.; Burrows, C. J.; White, H. S. Base-Excision Repair Activity of Uracil-DNA Glycosylase Monitored Using the Latch Zone of alpha-Hemolysin. *J. Am. Chem. Soc.* **2013**, *135* (51), 19347–19353.

(27) Wanunu, M.; Dadosh, T.; Ray, V.; Jin, J.; McReynolds, L.; Drndic, M. Rapid electronic detection of probe-specific microRNAs using thin nanopore sensors. *Nat. Nanotechnol.* **2010**, *5* (11), 807–14.

(28) Wang, Y.; Zheng, D.; Tan, Q.; Wang, M. X.; Gu, L.-Q. Nanopore-based detection of circulating microRNAs in lung cancer patients. *Nat. Nanotechnol.* **2011**, *6* (10), 668.

(29) Grosberg, A. Y.; Rabin, Y. DNA capture into a nanopore: interplay of diffusion and electrohydrodynamics. *J. Chem. Phys.* **2010**, *133* (16), 165102.

(30) Freedman, K. J.; Haq, S. R.; Fletcher, M. R.; Foley, J. P.; Jemth, P.; Edel, J. B.; Kim, M. J. Nonequilibrium capture rates induce protein accumulation and enhanced adsorption to solid-state nanopores. *ACS Nano* **2014**, *8* (12), 12238–12249.

(31) Meller, A.; Branton, D. Single molecule measurements of DNA transport through a nanopore. *Electrophoresis* **2002**, *23* (16), 2583–2591.

(32) Choi, G.; Song, D.; Shrestha, S.; Miao, J.; Cui, L. W.; Guan, W. H. A field-deployable mobile molecular diagnostic system for malaria at the point of need. *Lab Chip* **2016**, *16* (22), 4341–4349.

(33) Choi, G.; Prince, T.; Miao, J.; Cui, L. W.; Guan, W. H. Sample-to-answer palm-sized nucleic acid testing device towards low-cost malaria mass screening. *Biosens. Bioelectron.* **2018**, *115*, 83–90.

(34) Keller, N.; Grimes, S.; Jardine, P. J.; Smith, D. E. Single DNA molecule jamming and history-dependent dynamics during motor-driven viral packaging. *Nat. Phys.* **2016**, *12* (8), 757–761.

(35) Gershow, M.; Golovchenko, J. A. Recapturing and trapping single molecules with a solid-state nanopore. *Nat. Nanotechnol.* **2007**, *2* (12), 775–779.

(36) Patil, V.; Kulkarni, H. Comparison of confidence intervals for the Poisson mean: some new aspects. *REVSTAT-Statistical Journal* **2012**, *10* (2), 211–227.

(37) Subramanian, S.; Gomez, R. D. An Empirical Approach for Quantifying Loop-Mediated Isothermal Amplification (LAMP) Using *Escherichia coli* as a Model System. *PLoS One* **2014**, *9* (6), e100596.

(38) Takeuchi, S.; Kim, J.; Yamamoto, Y.; Hogue, H. H. Development of a high-quantum-efficiency single-photon counting system. *Appl. Phys. Lett.* **1999**, *74* (8), 1063–1065.

(39) Nouri, R.; Tang, Z.; Guan, W. Quantitative Analysis of Factors Affecting the Event Rate in Glass Nanopore Sensors. *ACS sensors* **2019**, DOI: [10.1021/acssensors.9b01540](https://doi.org/10.1021/acssensors.9b01540).

(40) Bell, N. A.; Thacker, V. V.; Hernández-Ainsa, S.; Fuentes-Perez, M. E.; Moreno-Herrero, F.; Liedl, T.; Keyser, U. F. Multiplexed ionic current sensing with glass nanopores. *Lab Chip* **2013**, *13* (10), 1859–1862.

(41) Choi, G.; Murphy, E.; Guan, W. Microfluidic Time-Division Multiplexing Accessing Resistive Pulse Sensor for Particle Analysis. *ACS sensors* **2019**, *4* (7), 1957–1963.